Paper 7

Computer Simulation of CO_2 Hydrate Growth

Trygve Buanes, Bjørn Kvamme, Atle Svandal

Journal of Crystal Growth, **287**, p491-494, (2006)

Available online at www.sciencedirect.com
SCIENCE DIRECT®
Journal of Crystal Growth 287 (2006) 491–494
JOURNAL OF CRYSTAL GROWTH
www.elsevier.com/locate/jcrysgro

Computer simulation of CO_2 hydrate growth

Trygve Buanes*, Bjørn Kvamme, Atle Svandal

Department of Physics and Technology, University of Bergen,Allégaten 55, N-5007 Bergen, Norway

Available online 6 January 2006

Abstract

In this work we present a model which is a hybrid of cellular automata and Monte Carlo to study the growth of CO_2 hydrate from aqueous solutions. We show that, depending on how large the driving forces are, the hydrate crystal may grow as compact structure or as a highly branched structure. Furthermore we show that the diffusion of CO_2 in the solution is the main limiting factor, unless the solution has a large supersaturation. Temperature effects are shown only to be important at large supersaturations.

PACS: 81.10.Aj; 81.10.Dn

Keywords: Al. Growth from solutions; B1. CO_2; B1. Gas hydrates

1. Introduction

Gas hydrates are crystalline structures of water with cavities filled by small molecules, e.g. CO_2 or methane. The presence of these guest molecules can stabilise the ice-like structure at temperatures well above the melting point of pure ice. Methane hydrate, or more generally hydrate from hydrocarbon mixtures, has been a problem for the oil and gas industry for decades. The degree of agglomeration of individual hydrate particles into massive hydrate blocks depends on the structure and surface properties of the hydrate particles. The kinetics of hydrate formation depends on the kinetics of mass transport, heat transport and the free energy changes related to the phase transition. The free energy change of the phase transition is the dominating factor on the structural development of the growing crystals. A crystal growing with small phase transition free energy differences will typically lead to crystals close to spherical while larger free energy differences will give rise to different kinds of branching. In this work we focus on CO_2 hydrate due to it's relevance in reservoir storage of CO_2. Many reservoirs that may be relevant for storage of CO_2 contain regions of temperature and pressure inside the hydrate stability zone. A rising CO_2 plume that enters these hydrate stability regions may form hydrate at the interface between the groundwater and the CO_2 phase. The resulting hydrate film will assist in reducing the leakage flux of CO_2 to the seafloor. But even if the examples presented in this work are for CO_2 we expect similar behaviour for other types of hydrate formers, like for instance natural gas, but then correspondingly shifted in temperature and pressure relative to the hydrate stability region for those specific hydrate forms.

2. Thermodynamics

We describe the thermodynamics using the free energy density $f(\phi, x_{CO_2}, T)$. Here ϕ is the order parameter describing the phase of the cell, $x_{CO_2} = n_{CO_2}/(n_{H_2O} + n_{CO_2})$ is the molar CO_2 fraction, and T is the temperature. In our model ϕ can only take the values 0 (liquid) and 1 (solid).

2.1. Liquid thermodynamics

The free energy density of the liquid is obtained by taking the contributions from pure water and from CO_2 in

*Corresponding author. Fax: +47 55 58 9440.
E-mail addresses: Trygve.Buanes@ift.uib.no (T. Buanes), Bjorn.Kvamme@ift.uib.no (B. Kvamme), Atle.Svandal@ift.uib.no (A. Svandal).

0022-0248/$ - see front matter © 2005 Elsevier B.V. All rights reserved.
doi:10.1016/j.jcrysgro.2005.11.074

infinite dilution, and adding to them a contribution to account for the mixing.

We do our simulations with a pressure of 150 bars and initial temperature in the liquid of 274 K. Under these conditions the aqueous solution is saturated at 3.3% CO_2 (obtained by extrapolating relevant data by Teng and Yamasaki [1]). Since we also want to do simulations with supersaturated solutions the liquid free energy density is extrapolated into the supersaturated region under the approximation that the activity coefficients follow the same concentration dependence as that fitted from saturated solutions.

2.2. Hydrate thermodynamics

The hydrate thermodynamics is based on a model by Kvamme and Tanaka [2] and van der Waals and Platteeuw [3]. The free energy density is given by

$$v_m f_s = x_{CO_2} g_{CO_2} + (1 - x_{CO_2}) g_w, \tag{1}$$

where v_m is the molar volume of the hydrate, and g_w and g_{CO_2} are partial molar free energies for water and CO_2 in the hydrate, respectively, given by

$$g_w = g_w^0 + RTv \log(1 - \theta), \tag{2}$$

$$g_{CO_2} = \Delta g^{inc} + RT \log\left(\frac{\theta}{1 - \theta}\right). \tag{3}$$

Here g_w^0 is the free energy density of water in empty hydrate, Δg^{inc} is the free energy of inclusion of gas molecules in the hydrate, $\theta = x_{CO_2}/v(1 - x_{CO_2})$ is the filling fraction of the cavities accessible to the CO_2 molecules, and v is the number of accessible cavities per water molecule.

3. Monte Carlo cellular automata

Cellular dynamical system models have been shown to be an efficient approach to computer simulations of crystal growth [4]. We propose a model which is a hybrid of Monte Carlo and cellular automata which we apply to study growth of CO_2 hydrate.

We do our simulations on a two-dimensional, quadratic grid. Each cell has a certain temperature, amount of H_2O and CO_2, and a phase. The phase can be either liquid or solid, but nothing in-between.

The ruling principle is free energy minimisation. We denote the free energy of a cell by $f(\phi, x_{CO_2}, T)$. Here ϕ is the order parameter describing the phase of the cell, $x_{CO_2} = n_{CO_2}/(n_{H_2O} + n_{CO_2})$ is the molar CO_2 fraction, and T is the temperature. The free energy minimisation is done through time steps involving solidification, and diffusion of mass and temperature.

3.1. Solidification

At each step a liquid cell with solid neighbours can change its phase with a certain probability depending on its temperature and CO_2 concentration. Let $\Delta f(x_{CO_2}, T)$ be the change in free energy density if a cell with molar CO_2 fraction x_{CO_2} and temperature T changes its phase from liquid to solid. Let r be a random number, $0 \leqslant r \leqslant 1$, then the cell solidifies if

$$r < e^{-\beta \Delta f(x_{CO_2}, T)[1 - \lambda(\Phi_n - 6)]}, \tag{4}$$

where $\Phi_n = \sum_n \omega_n \phi_n$ is a weighted sum over solid neighbours which is included to approximate the local interface curvature. We take $\omega_n = 2$ for nearest neighbours, $\omega_n = 1$ for next nearest neighbours and $\omega_n = 0$ otherwise. Since $\phi = 1$ for solid cells and $\phi = 0$ for liquid cells, the sum counts only solid neighbours. β is the characteristic energy scale for the solidification process.

3.2. Diffusion

Diffusion is done using a Monte Carlo implementation of Fick's law. At each time step one of the nearest neighbours is drawn randomly for each cell. The current

$$j_c = -D_c(\Delta n_{CO_2}(1 + \delta_c)), \tag{5}$$

where δ_c is a random number with a Gaussian distribution centred at 0, runs if

$$p < e^{-\beta \Delta f(j)}, \tag{6}$$

where p is a random number, $0 < p < 1$, $\Delta f(j)$ is the change in free energy for the two cells involved if the current j is allowed to run, and β^{-1} is the characteristic energy for the process.

The temperature diffusion is done in a similar fashion, but with $\beta = 0$. The current running is

$$j_T = -D_T(\Delta T(1 + \delta_T)), \tag{7}$$

where again δ_T is a random number with a Gaussian distribution centred at 0.

In our system $D_T \gg D_c$. Eqs. (5) and (7) requires both D_T and D_c to be less then 1 to work numerically. But to increase the computational efficiency we would like to have D_c close to 1. To be able to do this we modify Eq. (7) to read

$$j_T = -\frac{D_T}{m}(\Delta T + \delta_T), \tag{8}$$

such that $D_T/m < 1$ and run m temperature diffusion steps for each time step.

3.3. Length and time scale

To be able to extract some quantitative data we have to fix the length and time scale in the simulation. They are connected through the diffusion, but separately the scales are not explicitly given. Since a cell can be either solid or liquid, but noting in-between, we interpret the cell size to be of the same order as the thickness of the solid–liquid interface. For CO_2 hydrate this interface thickness is about 1 nm. The diffusion coefficient of CO_2 in water is $D_c = 10^{-9} m^2/s$. Thus by choosing the time scale to be

$\tau = \frac{1}{9} \times 10^{-9}$ s, the diffusion coefficient in dimensionless units is $D_c = \frac{1}{9}$.

4. Results

Since the mass transport is two orders of magnitude slower than the heat transport, the access to CO_2 from the aqueous solution is the main limiting factor on the hydrate growth. This is strongly reflected in both the growth rate, and in the morphology of the crystal. At low CO_2 concentrations the driving force is small, and the resulting crystal is compact. At higher CO_2 concentrations the driving force is larger, resulting in dendritic growth. The difference is shown in Fig. 1.

In Figs. 2 and 3 the linear size, measured as the maximal distance from the nucleation point, is plotted as a function of time. In addition there is square root fit to the data (for the supersaturated case only the first 2.5 μs is included in the fit). The growth from saturated solution shows excellent agreement with the fit, indicating that the growth is diffusion controlled. Also in the supersaturated solution the growth is in good agreement with a square root fit at early times, but at late times the linear size appears to approach a constant size. This is probably due to finite size effects in the simulation.

For growth from saturated solution, or with small supersaturation, both the growth rate and morphology of the resulting crystal is dominated by the mass transport, whereas the temperature has a minor effect. In Fig. 4 is the fraction of the system which is converted to hydrate shown for growth from a 4.5% CO_2 solution. The growing difference at late times is partly due to finite size effects in the simulation. Going to larger supersaturations the availability of CO_2 is sufficiently high such that the temperature then becomes the main limiting factor.

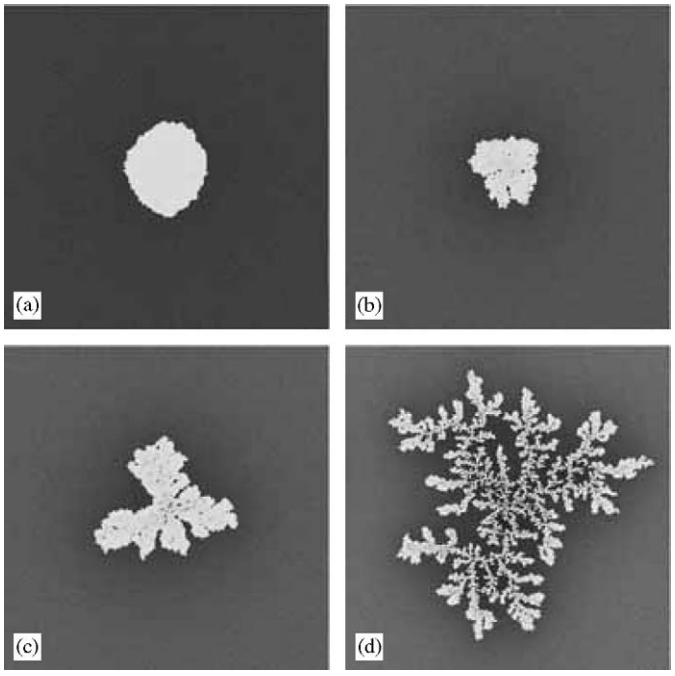

Fig. 1. Comparison of growth from a aqueous solution with different CO_2 concentrations, (a) 3.3% solution (saturated), snapshot after 61.1 μs, (b) 4% solution, snapshot after 11.1 μs, (c) 4.5% solution, snapshot after 11.1 μs, (d) 5% solution, snapshot after 2.2 μs. All simulations windows are 0.512 μm across.

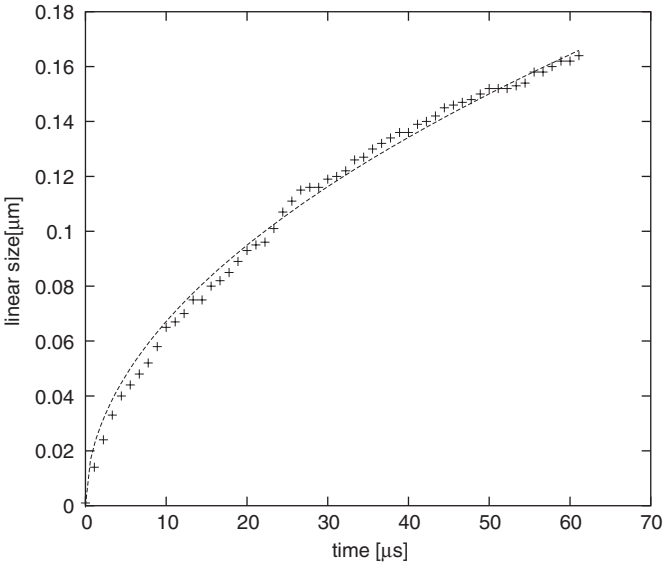

Fig. 2. Linear size of a crystal growing from a saturated solution (3.3% CO_2) plotted as a function of time. The dashed line is a square root fit to the data.

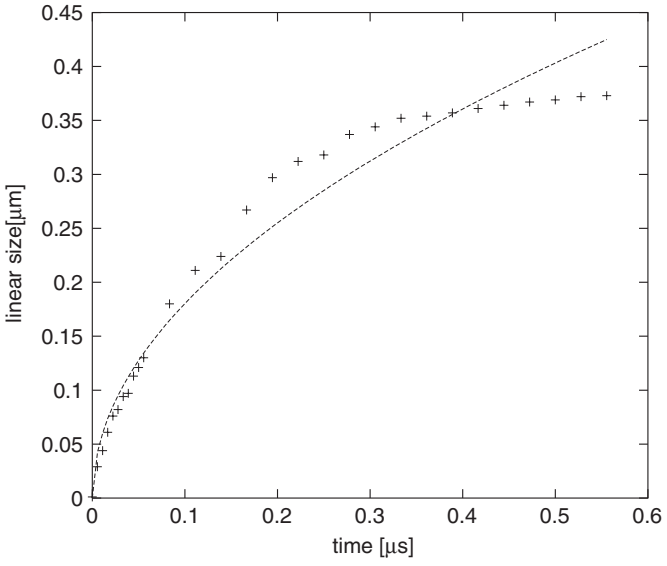

Fig. 3. Linear size of a crystal growing from a supersaturated solution (5% CO_2) plotted as a funciton of time. The dashed line is a square root fit to the data for times <2.5 μs.

5. Discussion

We have shown that using a model which is a hybrid of Monte Carlo and cellular automata we can simulate the

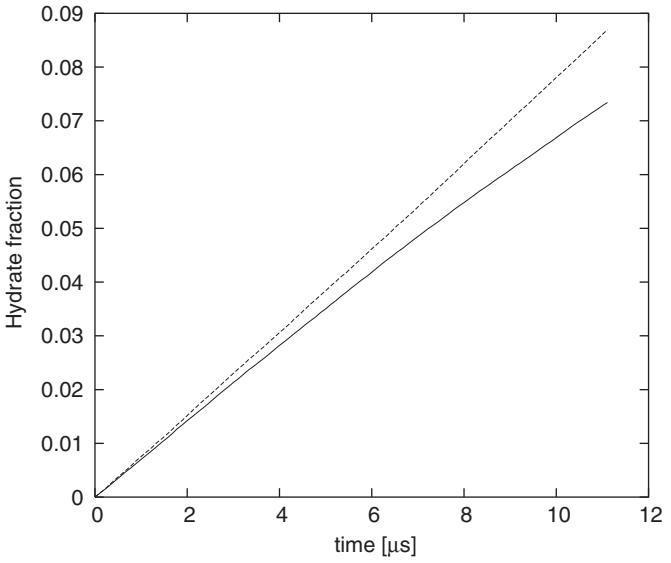

Fig. 4. Fraction of the system converted into hydrate with (solid line) and without (dashed line) temperature effects included.

growth of CO_2 hydrate giving qualitatively reasonable results. However, there are presently few experimental results on details of hydrate growth on such short time and length scales, so extrapolations of the results will probably be necessary to make quantitative comparisons with experiments.

Since the model only models growth, and not melting, it cannot be applied to systems in, or close to, equilibrium. However, if the system is far from equilibrium with conditions to provide steady growth, melting will be negligible and the model is expected to work.

Acknowledgements

This work has been supported financially by The Research Council of Norway and Hydro. We would also like to thank Joakim Hove, with whom the authors have had most fruitful discussions.

References

[1] H. Teng, A. Yamasaki, J. Chem. Eng. data 43 (1) (1998) 2.
[2] B. Kvamme, H. Tanaka, J. Phys. Chem. 99 (1995) 7114.
[3] J.H.v.d. Waals, J.C. Platteeuw, Adv. Chem. Phys. 2 (1959) 1.
[4] F. Liu, N. Goldenfeld, Phys. Rev. A 42 (2) (1990) 895.